

A novel experimental thrombotic myocardial infarction and primary angioplasty model in swine



Georgios Sideris^{1*}, MD, PhD; Nikolaos Magkoutis¹, MD, MSc; Sebastian Voicu², MD, PhD; Chantal Kang^{3,4}, PhD; Michel Bonneau^{3,4}, MB; Demetris Yannopoulos⁵, MD; Claire Bal Dit Sollier⁶, PhD; Jean-Guillaume Dillinger^{1,6}, MD, PhD; Natacha Berge⁶, MB; Jean-Philippe Brouland^{7,8}, MD, PhD; Patrick Henry¹, MD, PhD; Ludovic Drouet⁶, MD, PhD

1. Department of Cardiology - Inserm U942, Lariboisiere Hospital, AP-HP, Paris Diderot University, Paris, France; 2. Department of Medical and Toxicological Intensive Care - Inserm U1144, Lariboisiere Hospital, APHP, Paris Diderot University, Paris, France; 3. CR2I-INRA, Jouy en Josas, France; 4. Alpina European Research Institute - A.E.R.I, Archamps, France; 5. University of Minnesota, Cardiovascular Division, Minneapolis, MN, USA; 6. Thrombosis and Atherosclerosis Research Unit, Vessels and Blood Institute (IVS), Anticoagulation Clinic (CREATIF), Lariboisiere Hospital and Paris VII University EA 7334 REMES, Paris, France; 7. Pathology Department, Lariboisiere Hospital, Paris, France; 8. CHUV, Institut Universitaire de Pathologie, Lausanne, Switzerland

KEYWORDS

- adjunctive pharmacotherapy
- coronary occlusion
- myocardial infarction
- optical coherence tomography
- STEMI
- thrombus-containing lesion

Abstract

Aims: We sought to develop a reproducible animal model for acute myocardial infarction (AMI) in adult atherosclerosis-prone pigs.

Methods and results: A coil was placed in the right coronary artery or the left anterior descending artery in 26 downsized spontaneously hypercholesterolaemic pigs and left untreated until thrombotic occlusion. Then, we crossed the thrombotic occlusion with a guidewire, followed by predilatation, thrombus visualisation with optical coherence tomography (OCT) imaging and, finally, deployment of a stent and repeated OCT. After revascularisation, we calculated the index of microcirculatory resistance (IMR). After a feasibility phase (six animals), acute thrombotic occlusion was achieved in all 20 pigs. Eighteen animals were successfully revascularised and survived until sacrifice. Thrombus formation was confirmed by OCT, measurement of thrombin-antithrombin complexes and pathology examination. Myocardial necrosis was confirmed by troponin T elevation, myocardial staining and pathology examination. Distal thrombotic embolisation and microvascular obstruction were supported by increased IMR and pathology examination.

Conclusions: A porcine model of thrombotic occlusion AMI in miniaturised adult spontaneously atherosclerosis-prone pigs is feasible by percutaneous intracoronary placement of a coil. The reperfusion by angioplasty completed this model which mirrors human pathological conditions with myocardial infarction, necrosis and distal embolisation.

*Corresponding author: Department of Cardiology, Lariboisiere Hospital, 2 rue Ambroise Paré, 75010 Paris, France.
E-mail: georgios.sideris@aphp.fr

Abbreviations

AMI	acute myocardial infarction
BMW	Balance Middleweight
CAD	coronary artery disease
CVD	cardiovascular disease
EU	European Union
FDA	Food and Drug Administration
IMR	index of microcirculatory resistance
LAD	left anterior descending coronary artery
LM	left main
LV	left ventricle
MBG	myocardial blush grade
OCT	optical coherence tomography
PCI	percutaneous coronary intervention
RCA	right coronary artery
TAT	thrombin-antithrombin
TIMI	Thrombolysis In Myocardial Infarction
TTC	2,3,5-triphenyltetrazolium chloride
VF	ventricular fibrillation
VT	ventricular tachycardia

Introduction

Coronary artery disease (CAD) is the leading cause of morbidity and mortality in western society and a worldwide epidemic. Each year coronary vascular disease (CVD) causes over 3.9 million deaths in Europe including over 1.8 million deaths in the European Union (EU)¹⁻³. CVD causes 45% of all deaths in Europe and 37% in the EU³. Considering its personal and economic impact, the use of a sustainable and reproducible animal model that closely replicates the clinical and biochemical features of acute myocardial infarction (AMI) is required.

Several animal species are used to model AMI; however, swine have been proven superior for studies of AMI as well as ischaemic cardiomyopathy⁴. The coronary artery anatomy, size, structure and distribution make them suitable for preclinical research⁵. The porcine anatomy allows occlusion of the left anterior descending coronary artery (LAD), and therefore this is commonly used as a model of human CVD⁶. As in humans, the porcine LAD provides approximately half of the blood supply to the left ventricle (LV). Its occlusion results in an anteroapical, lateral and septal AMI of the LV that is similar in size and distribution to that in humans⁷. Therefore, LAD occlusion is the preferred model for preclinical studies, considering that it concerns the majority of human AMIs.

AMI in animal models using pigs and dogs is often developed by coronary ligation after surgical thoracotomy⁸. Several closed chest techniques have been developed in pigs to model non-reperused AMI, e.g., inflatable-detachable balloon occlusion⁹, flexible plug¹⁰, tungsten spiral¹¹, n-butyl cyanoacrylate injection¹², injection of embosene microspheres¹³, open-cell sponge¹⁴, ethanol¹⁵, thrombin¹⁶.

We present a reproducible and clinically relevant porcine model of AMI and reperfusion, with a thrombus component, similar to human AMI requiring primary angioplasty.

Methods

The study protocol was approved by the institute's Ethics Committee (Institut National de la Recherche Agronomique – INRA, ref: 12/048).

ANIMALS

We used a unique race of downsized adult pigs (familial hypercholesterolaemia Bretoncelles Meishan [FBM]) previously described, with spontaneous atherosclerosis, accelerated when fed with a proatherogenic diet¹⁷⁻²⁰. These pigs are derivative of the familial hypercholesterolaemic downsized (FHD) Rapacz pig colony. They are associated with several genetic defects, such as R84C mutation on the LDL receptor inducing a partial functional defect, and spontaneously develop atherosclerosis after 12 to 18 months¹⁷⁻¹⁹. At adulthood they weigh 40 to 70 kg. Under standard diet, they develop moderate hypercholesterolaemia (6±0.3 mmol/L) but no obvious coronary atherosclerosis¹⁹⁻²¹.

For our study, due to cost considerations, a regular balanced vegetarian diet was used, as major hypercholesterolaemia and patent atherosclerosis were not required for this protocol.

PREPARATION OF THE ANIMALS

We employed aseptic surgical conditions, using initial sedation with intramuscular ketamine 700 mg (Ketaset; Fort Dodge Animal Health, Fort Dodge, IA, USA) followed by inhaled 0.8-1.2% iso-fluorane. Pigs were intubated with a size 7.0 endotracheal tube and ventilated with room air, using a Narkomed ventilator (Narkomed, Telford, PA, USA) with volume control mode and a tidal volume of 10 mL/kg. The respiratory rate was adjusted to maintain arterial blood PaCO₂ at 40 mmHg and PaO₂ at around 80 mmHg. Surface electrocardiographic tracings were continuously recorded. All data were recorded with a digital recording system (BIOPAC MP150; BIOPAC Systems, Goleta, CA, USA). Central aortic blood pressure was recorded continuously with a micromanometer-tipped catheter (Mikro-Tip® Transducer; Millar Instruments, Houston, TX, USA) placed in the descending thoracic aorta.

All animals received an initial intravenous heparin bolus of 75 units/kg and 500 units every hour until the end of the protocol.

The ischaemia-reperfusion AMI model described here is a closed-chest approach using cardiac catheterisation techniques. Femoral access was obtained percutaneously in all animals.

EXPERIMENTAL MYOCARDIAL INFARCTION (Figure 1)

Under fluoroscopic guidance, a 5 Fr Amplatz 0.75 or a 5 Fr JR 3.5 guiding catheter was used in order to engage the ostium of the left main (LM) or the right coronary artery (RCA), respectively. In case of LAD occlusion, we used a non-hydrophilic 0.014-inch guidewire (aiming to improve the support), and intubated until the mid-LAD (after the first diagonal branch). After the selective intracoronary injection, we proceeded to distal wiring of the artery with a Balance Middleweight (BMW) J guidewire. We then placed a 0.038-inch (3-3.5×20-50 mm) Tornado® vascular coil (Cook Medical, Bloomington, IN, USA) (Figure 2A). The coil is placed

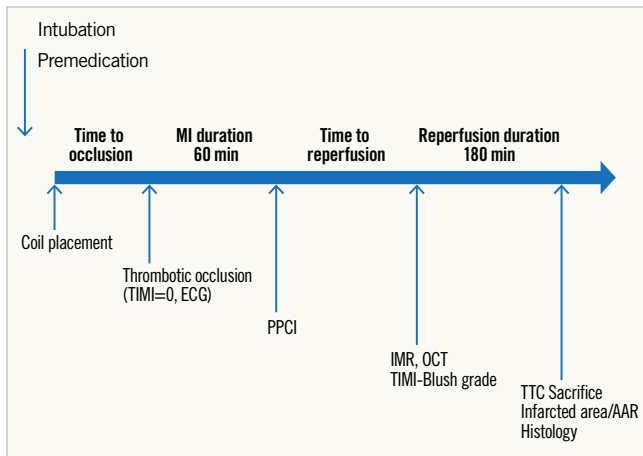


Figure 1. Study protocol. AAR: area at risk; IMR: index of microcirculatory resistance; MI: myocardial infarction; OCT: optical coherence tomography; PPCI: primary percutaneous coronary intervention; TIMI: Thrombolysis In Myocardial Infarction; TTC: triphenyltetrazolium chloride

via a microcatheter for progressive occlusion of all flow distal to either the first segment of the RCA or the first diagonal branch of the LAD²²⁻²⁴. By maintaining the patency of the first diagonal, a portion of the LV continues to receive blood perfusion. This provides well-defined border zones to the infarcted LV for comparative evaluation in preclinical studies. As a result, it reduces the fatalities during the procedure and creates fewer complications of congestive heart failure and more electrical stability after AMI.

After angiographic proof of total occlusion and 60 minutes duration of AMI (previously selected)²⁵, the lesion was crossed with a WHISPER® ES J wire (Abbott Vascular, Santa Clara, CA, USA). The lesion was subsequently predilated with a semi-compliant balloon and the thrombus was visualised with OCT imaging (**Figure 3A**, **Figure 3B**, **Figure 3C**). A stent was finally placed over the length of the lesion (proportional to the coil length and

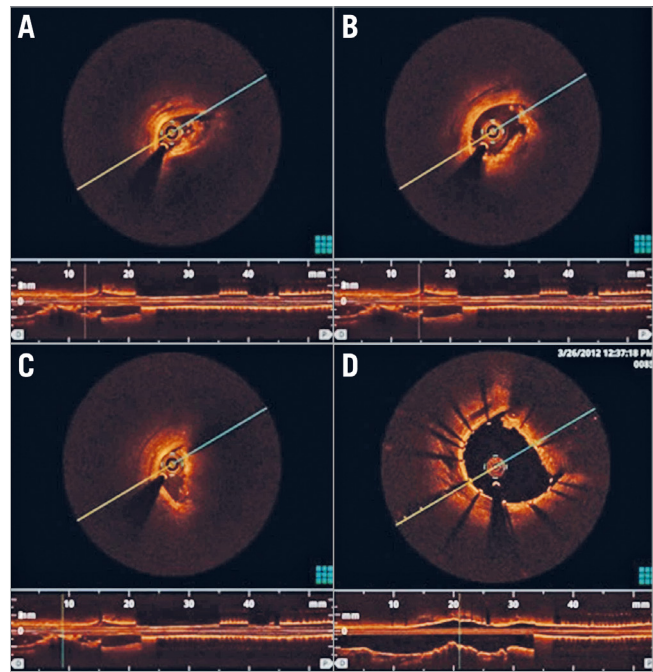


Figure 3. Thrombus confirmation by OCT. A), B), & C) Visualisation of intracoronary thrombus and coil after occlusion crossing and balloon dilation. D) Visualisation of stent deployment against coil with residual thrombus formation.

diameter) (**Figure 2B**) and OCT was repeated (**Figure 3D**). After stent deployment and intracoronary administration of nitroglycerine (200 mcg), we assessed the angiographic primary result with Thrombolysis In Myocardial Infarction (TIMI) flow grade²⁶ and myocardial blush grade (MBG)²⁷. Meanwhile, blood samples were taken at predetermined intervals to detect the burst of thrombin-antithrombin (TAT) complexes and troponin T levels before and after revascularisation. Troponin was assessed by the HS kit from Roche (ref:449815; Roche Diagnostics, Rotkreuz, Switzerland), chosen because pig troponin was recognised in this assay.

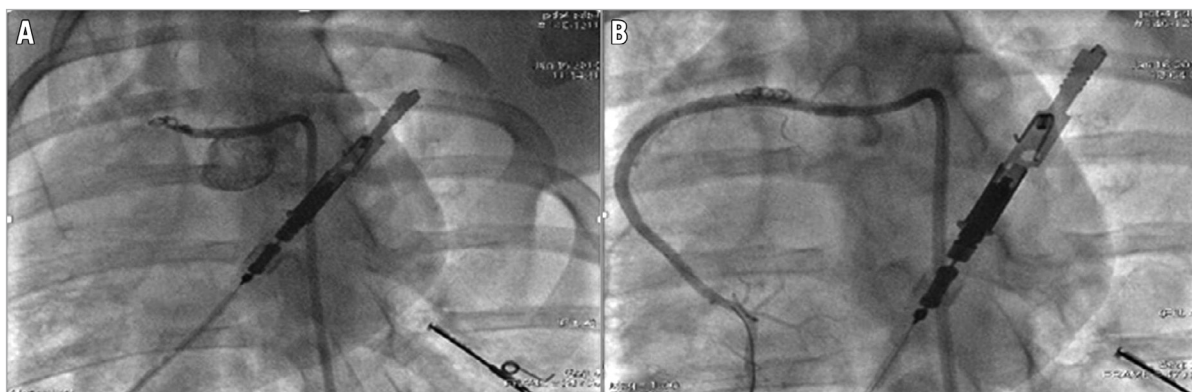


Figure 2. Experimental myocardial infarction. A) Selective injection of a contrast agent in the RCA of a pig (control). Placement of a 0.038-inch (3.5×25 mm) Tornado vascular coil (Cook Medical). B) Predilatation with a semi-compliant balloon and then placement of a stent. Angiographic control after the intracoronary administration of nitrate.

After revascularisation and stent deployment, we measured the index of microcirculatory resistance (IMR) in order to estimate the microcirculation state (PressureWire™ Certus™; St. Jude, St. Paul, MN, USA)^{28,29}. Since no reference values for IMR in this type of pig were available, we also measured baseline IMR in a separate group of five animals using papaverine for hyperaemia²⁹.

At the end of the protocol, *in situ* double staining with 1% Evans blue dye and 1% solution of 2,3,5-triphenyltetrazolium chloride (TTC) was performed to delineate areas at risk of ischaemia and infarcted areas, respectively³⁰. The injection of the dyes was universally lethal to the animals within 30 seconds. The Evans blue was infused upstream to the lesion and diffused in the myocardium not at risk. In the myocardium at risk, the TTC preparation allowed distinguishing the ischaemic from the non-ischaemic myocardium after coronary reopening.

HISTOLOGICAL PREPARATION OF THE SAMPLES

All specimens were fixed in 10% neutral buffered formalin for two weeks, dehydrated, embedded in paraffin and sliced in serial 4 µm sections. These sections were stained with haematoxylin eosin saffron.

For stented coronary arteries, the fixed material was embedded in resin and sectioned. After fixation in formalin, all the specimens were dehydrated in graded alcohol (70-100%), cleared in xylol and then impregnated stepwise with a mixture of xylol and methyl methacrylate. The tissue samples were then embedded in resin, and sections 300 µm thick were cut, ground to approximately 100 µm thickness, polished to an optical finish and stained with Stevenel's blue, and van Gieson's picrofuchsin.

Results

Among the 26 animals, the first six were included in the initial feasibility phase and 20 in the evaluation phase.

FEASIBILITY PHASE

The feasibility phase allowed us to establish several principles and technical details that were essential to the achievement of the thrombotic occlusion model.

Firstly, catheterisation of the coronary arteries must be performed using a 5 Fr guiding catheter. Indeed, the use of a 6 Fr catheter was attempted in two of the animals and was complicated by intractable episodes of ventricular fibrillation (VF) and cardiac arrest, probably due to the considerable size of the 6 Fr guiding catheters occluding the arteries and inducing electrical storm secondary to acute ischaemia.

Secondly, we determined the appropriate dosage of intravenous heparin to prevent uncontrolled thrombosis of the guiding catheter, but at the same time to allow enough coagulation for coil-induced thrombosis. We first tested a 100 IU/kg heparin bolus but, following this, the insertion of the coil was not accompanied by thrombus formation, and the vessel remained patent with TIMI 3 flow. Subsequently, the heparin dose was diminished to 50 IU/kg. This was complicated by thrombosis of the guiding catheter and

extensive thrombosis of the vessel. A heparin dose of 75 IU/kg was then used and proved to be optimal, allowing the thrombosis induced by the coil to take place and the target vessel to be completely (TIMI 0) occluded (up to 90 minutes), while avoiding excess thrombosis at other sites. This dosage was subsequently used in the evaluation phase.

The third major contribution in this phase was the crossing of the thrombotic "lesion" generated by the coil in the target vessel. We first attempted to cross the lesion using the "work-horse" BMW wire. Despite several attempts in two animals, the lesions could not be crossed. Then we used a hydrophilic wire, WHISPER ES. After several unsuccessful attempts, we employed a chronic total occlusion technique, improving support of the wire (using a Finecross® catheter [Terumo Corp., Tokyo, Japan]). If the lesion could still not be crossed, we used PROGRESS® 120, 140T, 200T (stiff) wires (Abbott Vascular). This consistently allowed us to cross the lesion and perform standard angioplasty and stent deployment, therefore completing the acute thrombosis model.

EVALUATION PHASE

After the feasibility phase, 20 animals were included in the evaluation phase of the model. Their general characteristics and total plasma cholesterol levels are presented in **Table 1**. Thrombotic occlusion was achieved in all 20 pigs. The site of the occlusion

Table 1. Characteristics of the animals (n=20) – evaluation phase.

Age (months)	15±3.3
Sex, female	9 (45%)
Weight (kg)	39±9.5
Total cholesterol concentration (mmol/L)	6.5±0.4
Occlusion site - RCA	11 (55%)
Occlusion site - LAD	9 (45%)
Time to occlusion (min)	69±29
Survival until PCI	20 (100%)
Time to reperfusion (min)	37±12.4
Number of wires (mean)	2±0.74
Number of balloons (mean)	2±0.5
TIMI post balloon PCI	1.9±0.3
TIMI 3 post PCI	16 (80%)
TIMI 2 post PCI	2 (10%)
TIMI 0-1 post PCI	2 (10%)
Survival at the end of PCI	18 (90%)
Animals with VT/VF until reperfusion	11 (55%)
Animals with VT/VF during or after reperfusion	15 (75%)
Defibrillation shocks until reperfusion	2.6±2
Defibrillation shocks after reperfusion	4.5±2.1
Stent diameter (mm)	3.3±0.4
Stent length (mm)	20±7
Heparin 75 IU/kg	20 (100%)
Data are number (%) or mean±SD. LAD: left anterior descending artery; RCA: right coronary artery; TIMI: Thrombolysis In Myocardial Infarction	

was the mid-LAD in nine animals and the proximal RCA in 11 animals. Eleven developed ventricular tachycardia (VT) and/or VF in the early phase of coronary occlusion before revascularisation was attempted, but they were successfully defibrillated. During or immediately after successful reperfusion, fifteen animals presented with VT/VF, also successfully defibrillated. Eighteen animals survived the whole protocol and TTC dye staining was successful. Two animals died of refractory VF due to unsuccessful revascularisation with TIMI flow 0-1 post percutaneous coronary intervention (PCI). Overall, our protocol had a 90% success rate in the evaluation phase.

Characteristics of the thrombotic occlusion and revascularisation procedures are shown in **Table 1**. All the steps of the thrombotic occlusion and reperfusion by angioplasty and stent implantation were successfully performed in the 20 included animals. The mean time required for coil deployment was seven minutes. The mean time interval between the coil placement and the ST-elevation myocardial infarction on the electrocardiogram with TIMI flow 0-1 (angiogram) was 69 minutes. An average of two wires were used to cross the thrombosed coil. Coronary angiography revealed TIMI flow grade 0 in all 20 pigs. The revascularisation time was 37 ± 12 minutes. TIMI flow grade 3 was achieved in 16 animals. No dissection was observed after the inflation of the balloon and the placement of the stent.

AMI was confirmed by electrocardiogram, biochemical, histological, macroscopic examination and TTC imaging in all animals. Data on the AMI characteristics are shown in **Table 2**. The IMR was elevated (mean value 43.7) in all animals after revascularisation and implantation of the stent, proving the myocardial damage and microvascular obstruction. The value of IMR observed in a separate group of five pigs of the same phenotype similar in age and weight was 9 ± 3 . The thrombotic component of the model was evaluated by assessment of the TAT complex measured at T0 (beginning of the procedure), T1 (just before revascularisation),

Table 2. Characteristics of the AMI (n=20) – evaluation phase.

Troponin T peak (ng ml ⁻¹)	42±10
IMR after AMI	43.7±12
TAT T0 (µg/l)	5±3
TAT T1 (µg/l)	8±5
TAT T2 (µg/l)	25±9
AAR weight (grams)	40±12
Infarction weight (grams)	18±7
Infarction to AAR (%)	45±16

Data are expressed as numbers (%) or mean±SD. AAR: area at risk found after triphenyltetrazolium chloride staining; IMR: index of microcirculatory resistance; TAT: thrombin-antithrombin complex

and T2 (the end of the reperfusion period). The results showing a large increase in TAT complex concentration are shown in **Table 2**. Troponin T measurements confirmed the AMI (mean value 42 ng/ml). Finally, Evans blue and TTC staining showed the AMI size and the ratio of infarcted myocardium/area at risk (**Table 2, Figure 4**). Histological assessment of the myocardial tissue showed large infarct areas in all animals (**Figure 5, Figure 6**) and the presence of distal embolisation.

The thrombus in the coronary epicardial artery at the site of coiling was of mixed composition: fibrin (clear areas in the thrombus, **Figure 5A**) imprisoning blood cells (dark areas in the thrombus, **Figure 5A**). Intraluminal thrombus formed after stenting was similar, of mixed composition, with fibrin areas (clear zone of the thrombus, **Figure 5B**) and areas imprisoning blood cells (dark area, **Figure 5B**). The sections represented in **Figure 5A** and **Figure 5B** are thick (100 µm) due to the presence of the coil; therefore, higher magnification examination was not possible. The emboli occluding the distal arterioles and capillaries (**Figure 6A, Figure 6B**) were of similar composition, formed of both platelets and leucocytes and fibrin imprisoning red blood cells. The microscopic examination

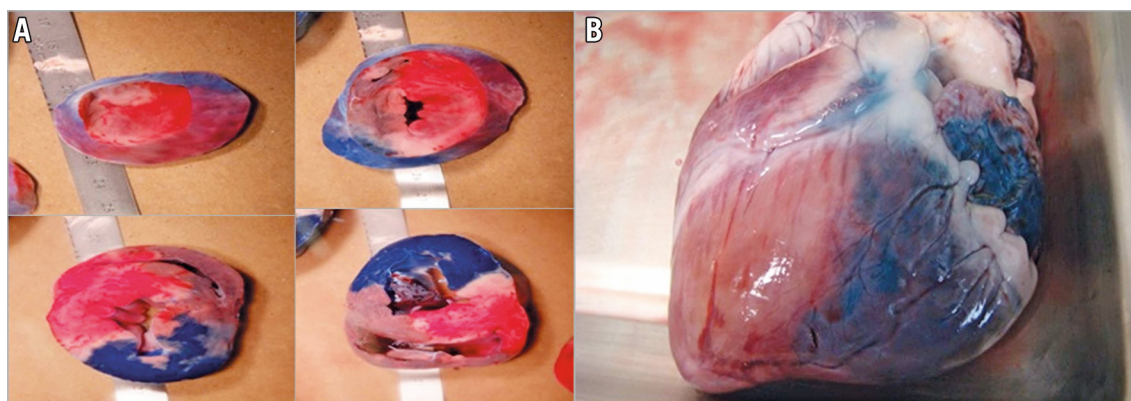


Figure 4. Myocardial infarction confirmation by TTC staining. A) Real photographs of LV slices. Blue stain (Evans blue) represents healthy myocardium. Red myocardium (TTC stained) represents non-infarcted myocardium. White myocardium (absence of TTC staining) represents myonecrosis. White and red areas represent the total AAR. B) Explanted heart showing stent position, AAR and blue stain healthy myocardium. AAR: area at risk

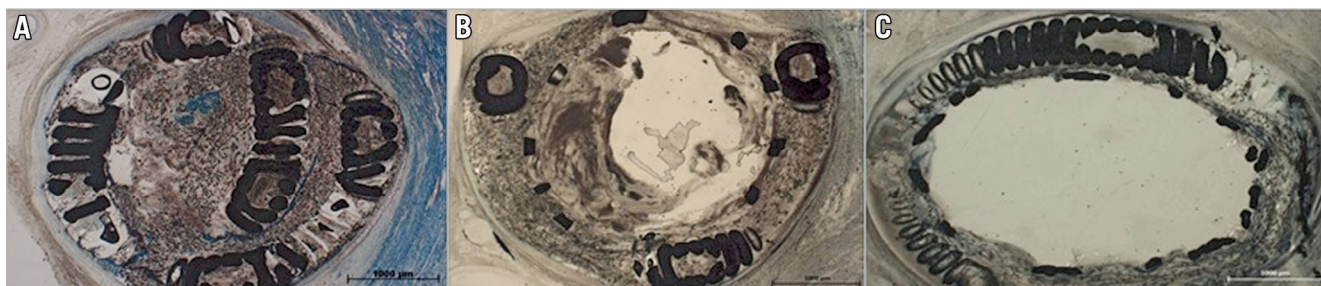


Figure 5. Coil and stent visualisation by histological examination. A) Complete coronary thrombotic occlusion on the deployed coil. B) After stenting some thrombotic material is in contact with the circulating blood. C) Successful reopening of the coil. The fully deployed stent constrains the thrombotic material and the coil outside of the stent at the inner surface of the arterial wall.

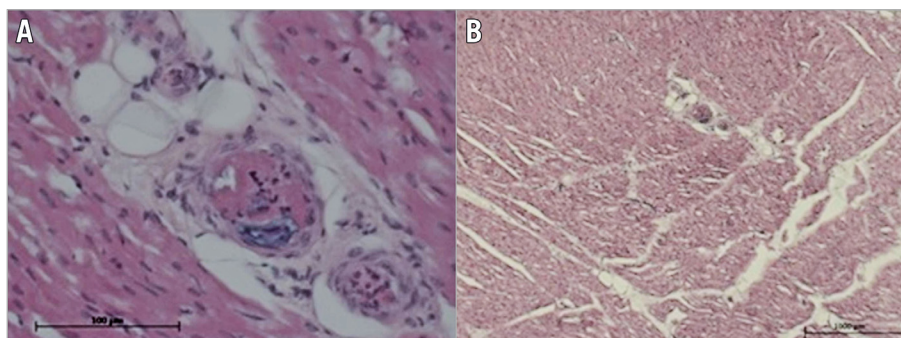


Figure 6. Thrombus distal embolisation confirmed by histological examination. A) High magnification of several arterioles embolised by thrombotic material formed by cellular material (platelets and leucocytes) and fibrin. B) Low magnification of at high risk myocardial tissues downstream of the thrombosed/stented epicardial coronary which shows multiple thromboembolic occlusions of the microvasculature.

of the tissues retrieved from the ischaemic zone at low magnification (10x) allowed the observation of five to eight arterioles per field, of which 18% (measured on 50 arterioles) contained thrombotic material, as described above.

Discussion

This model was effective in generating AMI, necrosis being confirmed by histopathological analysis and estimated at 45% of the area at risk. Our animal model is feasible, reproducible and closely simulates human acute coronary thrombosis and reperfusion/revascularisation. It allows the assessment of functional and histological coronary and myocardial damage. Our model mirrors the reperfusion techniques used in human AMI revascularisation.

Many occlusion models have been used in order to simulate the AMI pathophysiological mechanisms. Although the efficacy and the applicability of the existing methods are well established, the majority of the models available investigate only the effect of flow cessation by intracoronary balloon inflation or external ligation and therefore do not address a major component of AMI, namely intracoronary thrombosis. One of the rare models generating thrombotic occlusion was published by Ravn et al. This is an open chest model, using a vessel wall lesion and clamping. However, this model is less suitable for percutaneous reperfusion and long-term follow-up of the animals³¹.

Our model has several original aspects. We managed to create not only an arterial occlusion but also thrombus formation. The basic haemostatic and coagulation processes in pigs are similar to those in humans, and the anticoagulant and antiplatelet agents act similarly in both³². Intracoronary placement of the coil was the beginning of the thrombotic cascade generation that ended in the total thrombotic occlusion of the vessel, as in real-life human AMI. Thrombus generation was proven not only by the major increase in TAT levels from the beginning of the coronary occlusion until reperfusion, but also by endovascular OCT imaging. Indeed, direct visualisation of thrombus was possible using the OCT technique after predilatation of the occlusion with a balloon. This thrombotic feature could be useful for future evaluation of antiplatelet and anticoagulation drugs and different AMI pharmacologic treatment protocols.

Our revascularisation process is close to the therapeutic revascularisation encountered in human practice. Balloon inflation before stent implantation was followed by distal thrombus embolisation and thus diminished TIMI flow, blush and increased IMR. Distal embolisation of thrombus is a well-known process in human angioplasty and is responsible for the phenomenon of no-reflow which decreases the rate of success and effectiveness of the revascularisation. This microvascular obstruction is objectified by an increased IMR in our experimental study and

is documented in patients by IMR and magnetic resonance imaging (MRI), both of which have proven their prognostic value in human AMI studies^{28,29}. Our experimental model of AMI is capable of reproducing this phenomenon and opens up the perspective of experimental studies on pharmacological treatment of distal embolisation and microvascular obstruction. Distal embolisation was also demonstrated by the pathological analysis of the hearts. Although thrombotic occlusion guided by embozene microspheres is a well-established model of microvascular obstruction in the literature, it represents a model of non-reperused myocardial infarction¹³, contrary to our model which is capable of generating artery occlusion, thrombus formation and subsequent artery reperfusion.

Finally, our model includes a step of crossing of the artificially induced occlusive lesion, that is formed by the deployed coil and the thrombus formed essentially around the coil. The feasibility phase of the present study showed that crossing this complex lesion with a standard “workhorse” wire such as a BMW was not possible, and that more complex techniques, including the use of newer wires and Finecross catheters, were required to cross the lesion, representing an experimental model of complex angioplasty that may be used in the future to test angioplasty devices such as wires and microcatheters.

Limitations

Our model presents several limitations. It is relatively costly and time-consuming as it requires specialised interventions from the qualified veterinary technicians and interventional cardiologists as well as specialised equipment for mechanical ventilation, fluoroscopy PCI and imaging techniques.

The main limitation in this model is that thrombus formation in human AMI is induced by plaque rupture, while in our model thrombus was induced by the coil, exposing spaced synthetic fibres which potentiate a rapid thrombotic reaction. The thrombus is induced and stabilised by the coil (**Figure 5A**). Even after stenting, the exposed surface of the coil is highly thrombogenic and often induces a secondary thrombus formation inside the stent similar to that observed in humans (**Figure 5B**). When deployed, the stent will constrain the coil, its fibres and the initial thrombus on the vessel wall (**Figure 5C**). Even if the initial trigger is not atherosclerotic plaque rupture, all steps of reperfusion by angioplasty-stenting are similar to those in humans and seem relevant for translational research.

Another limitation to the translatability of the model is that atherosclerotic lesions are not present in the coronary tree, due to the standard regular diet of the pigs not allowing atherosclerosis to develop. It can be speculated that the animals we used (moderately hypercholesterolaemic) have some degree of endothelial dysfunction. However, using the same type of animal presenting with patent atherosclerosis may make the model even more translatable to human coronary disease¹⁷⁻²⁰. Nevertheless, the hypercholesterolaemic downsized pigs are rare and expensive, and atherosclerotic lesions require a relatively long time to develop.

The incidence of VF events was high, variable from one animal to the other, without any correlation between troponin levels and the number of VF events, suggesting that myocardial damage is mostly related to the thrombotic occlusion/reperfusion process.

Finally, the nature of the protocol, which required progressive thrombotic occlusion and a chronic total occlusion-like PCI technique, introduces two variables that decrease its reproducibility. Indeed, time to TIMI 0 after coil deployment and the time required for reperfusion may vary from one animal to another.

Conclusions

Our porcine model is feasible and reproducible utilising coil-induced coronary thrombosis. This acute thrombotic occlusion provides the substrate for acute reperfusion/revascularisation using an angioplasty technique similar to complex angioplasty in humans. This protocol represents a realistic model of human acute coronary occlusion and revascularisation and opens up new perspectives for experimental studies in the field of antithrombotic therapy of AMI and primary PCI techniques.

Impact on daily practice

The fact that our model mirrors real-life conditions of the manifestation and the treatment of AMI makes it useful in studies of different oncoming medications and materials. Precisely, it is the only method with progressive thrombotic occlusion, which permits studying antithrombotic regimens and primary PCI techniques as well as post-conditioning strategies.

Conflict of interest statement

The authors have no conflicts of interest to declare.

References

1. Thom T, Haase N, Rosamond W, Howard VJ, Rumsfeld J, Manolio T, Zheng ZJ, Flegal K, O'Donnell C, Kittner S, Lloyd-Jones D, Goff DC Jr, Hong Y, Adams R, Friday G, Furie K, Gorelick P, Kissela B, Marler J, Meigs J, Roger V, Sidney S, Sorlie P, Steinberger J, Wasserthiel-Smoller S, Wilson M, Wolf P; American Heart Association Statistics Committee and Stroke Statistics Subcommittee. Heart disease and stroke statistics--2006 update: a report from the American Heart Association Statistics Committee and Stroke Statistics Subcommittee. *Circulation*. 2006; 113:e85-151.
2. Heidenreich PA, Trogon JG, Khavjou OA, Butler J, Dracup K, Ezekowitz MD, Finkelstein EA, Hong Y, Johnston SC, Khera A, Lloyd-Jones DM, Nelson SA, Nichol G, Orenstein D, Wilson PW, Woo YJ; American Heart Association Advocacy Coordinating Committee; Stroke Council; Council on Cardiovascular Radiology and Intervention; Council on Clinical Cardiology; Council on Epidemiology and Prevention; Council on Arteriosclerosis; Thrombosis and Vascular Biology; Council on Cardiopulmonary; Critical Care; Perioperative and Resuscitation; Council on Cardiovascular Nursing; Council on the Kidney in Cardiovascular

Disease; Council on Cardiovascular Surgery and Anesthesia, and Interdisciplinary Council on Quality of Care and Outcomes Research. Forecasting the future of cardiovascular disease in the United States: a policy statement from the American Heart Association. *Circulation*. 2011;123:933-44.

3. Wilkins E, Wilson L, Wickramasinghe K, Bhatnagar P, Leal J, Luengo-Fernandez R, Burns R, Rayner M, Townsend N (2017). European Cardiovascular Disease Statistics 2017. European Heart Network, Brussels. <http://www.ehnheart.org/images/CVD-statistics-report-August-2017.pdf>

4. Swindle MM. *Swine in the Laboratory: Surgery, Anesthesia, Imaging, and Experimental Techniques*. Boca Raton, FL, USA: CRC Press (Taylor & Francis Group); 2007.

5. Dondelinger RF, Ghysels MP, Brisbois D, Donkers E, Snaps FR, Saunders J, Devière J. Relevant radiological anatomy of the pig as a training model in interventional radiology. *Eur Radiol*. 1998;8:1254-73.

6. Amado LC, Saliaris AP, Schuleri KH, St John M, Xie JS, Cattaneo S, Durand DJ, Fitton T, Kuang JQ, Stewart G, Lehrke S, Baumgartner WW, Martin BJ, Heldman AW, Hare JM. Cardiac repair with intramyocardial injection of allogeneic mesenchymal stem cells after myocardial infarction. *Proc Natl Acad Sci USA*. 2005;102:11474-9.

7. Ortiz-Pérez JT, Meyers SN, Lee DC, Kansal P, Klocke FJ, Holly TA, Davidson CJ, Bonow RO, Wu E. Angiographic estimates of myocardium at risk during acute myocardial infarction: validation study using cardiac magnetic resonance imaging. *Eur Heart J*. 2007;28:1750-8.

8. Litvak J, Siderides LE, Vineberg AM. The experimental production of coronary artery insufficiency and occlusion. *Am Heart J*. 1957;53:505-18.

9. Garner D, Ginzton LE, Jagels G, Laks MM. A new technique for producing myocardial infarction using coronary artery balloon occlusion. *Cardiovasc Res*. 1988;22:42-6.

10. Herr MD, McInerney JJ, Copenhaver GL, Morris DL. Coronary artery embolization in closed-chest canines using flexible radiopaque plugs. *J Appl Physiol*. 1988;64:2236-9.

11. Peukert D, Laule M, Kaufels N, Schnorr J, Taupitz M, Hamm B, Dewey M. A minimally invasive method for induction of myocardial infarction in an animal model using tungsten spirals. *Int J Cardiovasc Imaging*. 2009;25:529-35.

12. Matos GF, Hammadeh R, Francois C, McCarthy R, Leya F. Controlled myocardial infarction induced by intracoronary injection of n-butyl cyanoacrylate in dogs: a feasibility study. *Catheter Cardiovasc Interv*. 2005;66:244-53.

13. Varga-Szemes A, Kiss P, Brott BC, Wang D, Simor T, Elgavish GA. Embozene™ microspheres induced nonreperfused myocardial infarction in an experimental swine model. *Catheter Cardiovasc Interv*. 2013;81:689-97.

14. Reffelmann T, Sensebat O, Birnbaum Y, Stroemer E, Hanrath P, Uretsky BF, Schwarz ER. A novel minimal-invasive model of chronic myocardial infarction in swine. *Coron Artery Dis*. 2004;15:7-12.

15. Kim W, Jeong MH, Sim DS, Hong YJ, Song HC, Park JT, Ahn YK. A porcine model of ischemic heart failure produced by intracoronary injection of ethyl alcohol. *Heart Vessels*. 2011;26:342-8.

16. Osipov RM, Robich MP, Feng J, Clements RT, Liu Y, Glazer HP, Wagstaff J, Bianchi C, Sellke FW. Effect of thrombin fragment (TP508) on myocardial ischemia-reperfusion injury in hypercholesterolemic pigs. *J Appl Physiol*. 2009;106:1993-2001.

17. Thim T, Hagensen MK, Drouet L, Bal Dit Sollier C, Bonneau M, Granada JF, Nielsen LB, Paaske WP, Bøtker HE, Falk E. Familial hypercholesterolaemic downsized pig with human-like coronary atherosclerosis: a model for preclinical studies. *EuroIntervention*. 2010;6:261-8.

18. Thim T, Hagensen MK, Wallace-Bradley D, Granada JF, Kaluza GL, Drouet L, Paaske WP, Bøtker HE, Falk E. Unreliable assessment of necrotic core by virtual histology intravascular ultrasound in porcine coronary artery disease. *Circ Cardiovasc Imaging*. 2010;3:384-91.

19. Thim T, Hagensen MK, Hørlyck A, Kim WY, Niemann AK, Thrysøe SA, Drouet L, Paaske WP, Bøtker HE, Falk E. Wall shear stress and local plaque development in stenosed carotid arteries of hypercholesterolemic minipigs. *J Cardiovasc Dis Res*. 2012;3:76-83.

20. Prescott MF, Hasler-Rapacz J, von Linden-Reed J, Rapacz J. Familial hypercholesterolemia associated with coronary atherosclerosis in swine bearing different alleles for apolipoprotein B. *Ann N Y Acad Sci*. 1995;748:283-92.

21. Poulsen CB, Al-Mashhadi AL, von Wachenfeldt K, Bentzon JF, Nielsen LB, Al-Mashhadi RH, Thygesen J, Tolbod L, Larsen JR, Frøkiær J, Tawakol A, Vucic E, Fredrickson J, Baruch A, Freundus B, Robertson AK, Moestrup SK, Drouet L, Falk E. Treatment with a human recombinant monoclonal IgG antibody against oxidized LDL in atherosclerosis-prone pigs reduces cathepsin S in coronary lesions. *Int J Cardiol*. 2016;215:506-15.

22. Sideris G, Magkoutis N, Sharma A, Rees J, McKnite S, Caldwell E, Sarraf M, Henry P, Lurie K, Garcia S, Yannopoulos D. Early coronary revascularization improves 24h survival and neurological function after ischemic cardiac arrest. A randomized animal study. *Resuscitation*. 2014;85:292-8.

23. Kumar A, Santana D, Jenkins LA. Closure of a giant saphenous vein graft aneurysm with embolization coil. *Cardiol Res Pract*. 2009;2009:748272.

24. Jacobs BL, Maranchie JK. Embolization with Tornado coils to control bleeding from an arterioureteral fistula. *Can J Urol*. 2007;14:3770-2.

25. Suzuki Y, Lyons JK, Yeung AC, Ikeno F. In vivo porcine model of reperfused myocardial infarction: in situ double staining to measure precise infarct area/area at risk. *Catheter Cardiovasc Interv*. 2008;71:100-7.

26. TIMI Study Group. The Thrombolysis in Myocardial Infarction (TIMI) trial. Phase I findings. *N Engl J Med*. 1985;312:932-6.

27. Gibson CM, de Lemos JA, Murphy SA, Marble SJ, Dauterman KW, Michaels A, Barron HV, Antman EM; TIMI Study

Group. Methodologic and clinical validation of the TIMI myocardial perfusion grade in acute myocardial infarction. *J Thromb Thrombolysis*. 2002;14:233-7.

28. Fearon WF, Low AF, Yong AS, McGeoch R, Berry C, Shah MG, Ho MY, Kim HS, Loh JP, Oldroyd KG. Prognostic value of the Index of Microcirculatory Resistance measured after primary percutaneous coronary intervention. *Circulation*. 2013;127:2436-41.

29. Fiarresga A, Selas M, Oliveira E, Cavaco-Gonçalves S, Cacula D, Carrapiço B, Cardim N, Cruz Ferreira R. Invasive assessment of the coronary microcirculation using the index of microcirculatory resistance: description and validation of an animal model. [Article in English, Portuguese]. *Rev Port Cardiol*. 2014;33:207-12.

30. Yannopoulos D, Zviman M, Castro V, Kollandaivelu A, Ranjan R, Wilson RF, Halperin HR. Intra-cardiopulmonary resuscitation hypothermia with and without volume loading in an ischemic model of cardiac arrest. *Circulation*. 2009;120:1426-35.

31. Ravn HB, Moeldrup U, Brookes CI, Ilkjaer LB, White P, Chew M, Jensen L, Johnsen S, Birk-Soerensen L, Hjortdal VE. Intravenous magnesium reduces infarct size after ischemia/reperfusion injury combined with a thrombogenic lesion in the left anterior descending artery. *Arterioscler Thromb Vasc Biol*. 1999;19:569-74.

32. Roussi J, André P, Samama M, Pignaud G, Bonneau M, Laporte A, Drouet L. Platelet functions and haemostasis parameters in pigs: absence of side effects of a procedure of general anaesthesia. *Thromb Res*. 1996;81:297-305.